Origin of NMR shielding in fluorides

Robert Laskowski and Peter Blaha
Institute of Materials Chemistry, Vienna University of Technology, Getreidemarkt 9/165TC, A-1060 Vienna, Austria
(Received 2 March 2012; published 15 June 2012)

In this work, we analyze in detail the relation between electronic structure and fluorine nuclear magnetic resonance (NMR) shielding in a series of solid state alkali fluorides (LiF, NaF, KF, RbF, and CsF). For that purpose, we use solid-state NMR calculations implemented in the density functional theory full potential WIEN2K code (APW + lo). Both measurements and calculations show that the NMR shielding varies across the series by approximately 200 ppm. We focus our discussion on an explanation of the origin of the observed trend, and we show that the variation is mainly determined by contributions from "semicore" metal-*p* and valence F-*p* bands. More specifically, the trend in fluorine shielding can be related to the small but significant change in the hybridization of these states. A second important ingredient determining the value of the shielding is the presence and position of metal-*d* states in the unoccupied part of the Kohn-Sham bands. Although the present analysis has been demonstrated for the ^{19}F nucleus in alkali fluorides, the main results are more general and can explain similar trends observed in other solids and for other nuclei.

DOI: 10.1103/PhysRevB.85.245117 PACS number(s): 71.45.Gm, 71.15.−m, 76.60.Cq

I. INTRODUCTION

Nuclear magnetic resonance (NMR) spectroscopy measures the response of a material to an external magnetic field by detecting the transition energies related to the reorientation of the nuclear magnetic moment.[1] Due to the presence of electrons, the magnetic field at the nucleus differs from the external field, resulting in so called NMR shielding. The difference is related to the induced electric current, which depends strongly on the atomic and electronic structure of the investigated material. Therefore, NMR measurements provide indirect information about these properties. Nowadays, NMR is routinely used for studying the structures of molecules and solids.[2] In the case of small molecules and H or C nuclei, the interpretation of the measured spectra is often based on a set of empirical rules that model the indirect relation between the molecular structure and the NMR spectra.[3] However, for other (heavier) nuclei, or large molecules and solids, the response depends on the details of the electronic structure in a rather complicated way,[4–8] therefore the interpretation of the experimental data is a rather difficult task.[9–11] Even by means of *ab initio* calculations, which are undoubtedly helpful, one can at best reproduce the experimental spectra allowing an assignment to specific atomic sites,[12,13] but so far it is basically not understood why the NMR shielding is smaller or larger in one compound than in another.

The aim of the present work is to perform a detailed analysis of the relation between electronic structure and NMR shielding. An understanding of this relation will certainly enhance the value of NMR chemical shift measurements as a method yielding valuable insight into the chemical bonding of a material. Years ago, a similar breakthrough was made possible for quadrupole splitting, where the understanding of the origin of the electric field gradient changed the interpretation from a "point charge" to a "chemical bonding" point of view.[14]

As a specific example, we analyze the trend of fluorine NMR shielding in a series of solid-state alkali fluorides (LiF, NaF, KF, RbF, and CsF). It has been observed that the NMR shift changes by as much as 200 ppm (Ref. 12) between LiF and CsF despite the fact that they have an identical crystal structure and basically similar, highly ionic bonding. Figure 1 presents measured[12] and calculated isotropic NMR chemical shifts. The agreement is reasonable but suffers a bit from the well known errors of present semilocal functionals, which leads in a comparison between theory and experiment to slopes other than 1.[12,15] It has already been noticed that the chemical shifts in the series correlate to some extent with electronegativities and polarizabilities[16] or ionic radii[17,18] of the metal atoms. NMR shielding for those compounds has also been calculated before by others[12,19,20] and by us,[21] but the reason for this strong variation has not been discussed and is not yet understood. Similar trends were observed for series other than alkali fluorides, e.g., alkali earth fluorides[12] or alkali earth oxides.[15] Our final conclusions, formulated for alkali fluorides, should also hold for those cases.

II. THEORETICAL APPROACH

Before presenting the results, we outline our approach to calculate the NMR shielding. The method is based on a linear-response theory widely used for NMR calculations in solids.[22–24] A detailed description of our implementation into WIEN2K (Ref. 25) was published recently.[21] The shielding tensor $\overleftrightarrow{\sigma}$ is a proportionality factor between the induced magnetic field $\mathbf{B}_{\rm ind}$ measured at the nucleus at site $\mathbf{R}$ and the external field $\mathbf{B}$:

$$\mathbf{B}_{\rm ind}(\mathbf{R}) = -\overleftrightarrow{\sigma}(\mathbf{R})\mathbf{B}. \tag{1}$$

In this work, we discuss properties of the isotropic shielding (IS), which is given by $\sigma(\mathbf{R}) = \mathrm{Tr}[\overleftrightarrow{\sigma}(\mathbf{R})]$. The experimentally measured chemical shift δ can be obtained only with respect to some reference compound ($CFCl_3$ in the case of fluorine), and therefore $\delta(\mathbf{R}) = \sigma_{\rm ref} - \sigma(\mathbf{R})$. The induced field $\mathbf{B}_{\rm ind}$ is evaluated by integrating the induced current $\mathbf{j}_{\rm ind}(\mathbf{r})$ according to the Biot-Savart law:

$$\mathbf{B}_{\rm ind}(\mathbf{R}) = \frac{1}{c}\int d^3r\, \mathbf{j}_{\rm ind}(\mathbf{r}) \times \frac{\mathbf{R}-\mathbf{r}}{|\mathbf{r}-\mathbf{R}|^3}\,. \tag{2}$$

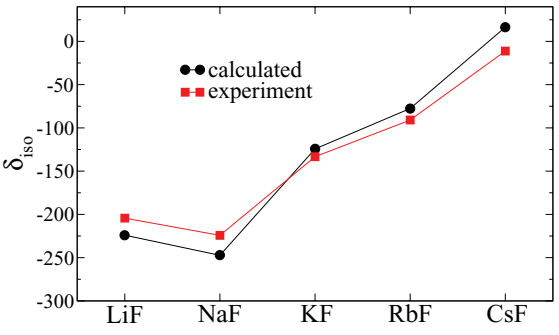

FIG. 1. (Color online) Calculated and measured[12] isotropic NMR chemical shifts δ_{iso} at the fluorine nucleus in the alkali fluoride series. The calculated absolute isotropic shielding at the fluorine in the reference compound $CFCl_3$ is 159 ppm.

For nonmagnetic and insulating materials, only the orbital motion of the electrons contributes to $\mathbf{j}_{ind}(\mathbf{r})$. The induced current is calculated in the framework of perturbation theory, where the first-order perturbation of the Hamiltonian in the symmetric gauge is

$$H^{(1)} = \frac{1}{2c}\mathbf{r} \times \mathbf{p} \cdot \mathbf{B}. \tag{3}$$

Within density functional theory (DFT), the current density is evaluated as a sum of the expectation values of the current operator running over the occupied Kohn-Sham (KS) states:

$$\mathbf{J}(\mathbf{r}') = -\frac{\mathbf{p}|\mathbf{r}'\rangle\langle\mathbf{r}'| + |\mathbf{r}'\rangle\langle\mathbf{r}'|\mathbf{p}}{2} - \frac{\mathbf{B}\times\mathbf{r}'}{2c}|\mathbf{r}'\rangle\langle\mathbf{r}'|. \tag{4}$$

The expression for the induced current involves only the first-order terms with respect to the external field $\mathbf{B}$:

$$\mathbf{j}_{ind}(\mathbf{r}') = \sum_o \left[\left\langle\Psi_o^{(1)}\middle|\mathbf{J}^{(0)}(\mathbf{r}')\middle|\Psi_o^{(0)}\right\rangle + \left\langle\Psi_o^{(0)}\middle|\mathbf{J}^{(0)}(\mathbf{r}')\middle|\Psi_o^{(1)}\right\rangle + \left\langle\Psi_o^{(0)}\middle|\mathbf{J}^{(1)}(\mathbf{r}')\middle|\Psi_o^{(0)}\right\rangle\right], \tag{5}$$

where $\Psi_o^{(0)}$ is an unperturbed (KS) occupied orbital. $J^0(\mathbf{r}')$ is the paramagnetic part of the current operator [the first term in Eq. (4)], $J^1(\mathbf{r}')$ is the diamagnetic component of the current operator [the second term in Eq. (4)]. $\Psi_o^{(1)}$ is the first-order perturbation of $\Psi_o^{(0)}$ with respect to $H^{(1)}$ expressed using a standard perturbation theory formula,

$$\left|\Psi_o^{(1)}\right\rangle = \sum_e \left|\Psi_e^{(0)}\right\rangle \frac{\left\langle\Psi_e^{(0)}\middle|H^{(1)}\middle|\Psi_o^{(0)}\right\rangle}{\epsilon - \epsilon_e}, \tag{6}$$

with the sum running over the empty (unoccupied) KS orbitals. Here we should stress that Eq. (5) is used as a reference formula in order to discuss the physics, while the actual formulas specific to the WIEN2K implementation are derived in Ref. 21. We stress that contrary to the reference formula Eq. (5), our actual implementation is gauge-invariant and the results do not depend on the choice of the unit cell origin.

The calculations presented in this work have been performed using the WIEN2K code[25] and are based on the augmented plane wave plus local orbital (APW + lo) method and the DFT with PBE (Ref. 26) exchange correlation functional. Within this method, the unperturbed wave functions as well as their first-order perturbations are expressed using plane waves in the interstitial region and an atomiclike representation inside the atomic spheres S_α:

$$\Psi_{n,\mathbf{k}}(\mathbf{r}) = \begin{cases} \frac{1}{\sqrt{\Omega}}\sum_{\mathbf{G}} C_G^{n,\mathbf{k}} e^{i(\mathbf{G}+\mathbf{k})\cdot\mathbf{r}}, & \mathbf{r}\in I \\ \sum_{lm} W_{lm}^{n,\alpha,\mathbf{k}}(r)Y_{lm}(\hat{r}), & \mathbf{r}\in S_\alpha. \end{cases} \tag{7}$$

In contrast to standard ground-state calculations, IS calculations require an extended basis set inside the spheres, which is achieved by supplying additional local orbitals as described in Ref. 21. To ensure the full convergence, we use ten extra local orbitals for $l = 0,1,2$. For other computational parameters, the standard values lead to well-converged results. Specifically, the plane-wave cutoff was set according to $RK_{max} = 7$ ($R =$ 1.8 a.u. is the sphere radii of fluorine atom, K_{max} is the plane-wave momentum cutoff), and k-point sampling was done with an $8 \times 8 \times 8$ mesh.

III. RESULTS

The electronic structure of the alkali fluorides is characterized by narrow metal and fluorine, s and p bands. The density of states (DOS) calculated for CsF is presented in Fig. 2. The topmost valence band (below 0 eV) is dominated by F-2p character. The width of this band depends on the unit cell volume; it varies between 3.0 eV for LiF and 1.0 eV for CsF. The separation between the metal-p and F-p states varies between 20 eV for NaF and 5 eV for CsF. Although both the F-p and metal-p bands are dominated by their corresponding main component, some hybridization between them is present and shows up in the corresponding partial DOS (Fig. 2). F-2s and semicore metal-s bands lie at much lower energies and thus hardly show any interaction with other orbitals.

As a first step in our analysis, we partition the IS into contributions from the metal and F bands. The calculated total and partial IS are given in Table I. First, we notice that the majority of the IS comes from the current inside the fluorine atomic sphere ($R_{MT}^F = 1.8$ a.u.), while the rest of the unit cell volume contributes only a few ppm. As expected, the core contribution to the fluorine IS is large, but it is constant across the series. Similarly, the contribution from the F-s band shows only a small variation between 24 and 27 ppm. The trend in the NMR shielding is fully determined by the metal-p and F-2p bands. The part of the shielding related to the metal-p band increases from nearly 0 ppm for NaF to 100 ppm for CsF, whereas the contribution from the F-p band decreases from about 53 ppm for LiF to −284 ppm for CsF.

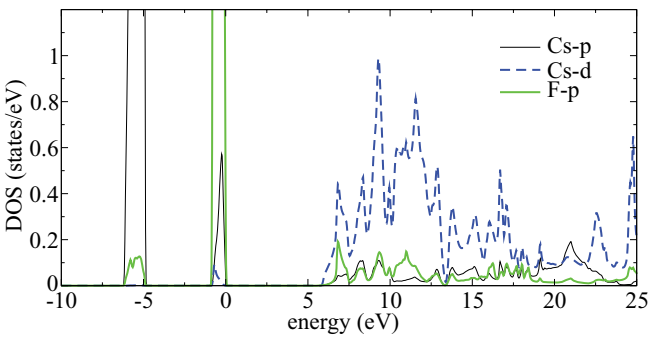

FIG. 2. (Color online) The partial density of states calculated for CsF.

TABLE I. Band-resolved contribution to ^{19}F NMR isotropic shielding (ppm). The *sphere* contribution to the *total* NMR IS is evaluated by integrating the induced current in the F sphere only. The *core* contribution is related to the spherical core charge density. The contributions from F-p, metal-p, and F-s bands are evaluated by including only those bands in the evaluation of the induced current.

	LiF	NaF	KF	RbF	CsF
total	383.0	406.3	283.3	236.6	142.6
sphere	381.8	404.5	281.8	234.4	138.3
core	306.4	306.4	306.4	306.4	306.4
F-s band	24.3	24.2	25.6	26.1	27.5
metal-p band		0.0	20.0	48.4	101.8
F-p band	52.9	76.3	− 67.0	− 139.6	− 284.31

In order to understand the origin of these variations, we decompose the IS with respect to s, p, and d components of the ground-state wave functions $\Psi_o^{(0)}$ and its first-order perturbation $\Psi_o^{(1)}$ defined in Eq. (6). The major contributions are listed in Table II and can be compared to the total IS as given in Table I. The notation $\Psi_o^{(0,1)}|_{\alpha,l}$ indicates that the induced current has been calculated using only the selected angular momentum l component of $\Psi_o^{(0)}$ or $\Psi_o^{(1)}$ inside the atomic sphere α. For the F-2s band, the entire shielding comes from $\Psi_o^{(0)}|_{\mathrm{F},l=0}$ and $\Psi_o^{(1)}|_{\mathrm{F},l=1}$ character, which is related to the fact that only the $l = 1$ component of the induced current contributes to the IS.

In the metal-p band, most of the charge is of course localized at the metal atom, but only the small F-2p character ($\Psi_o^{(0)}|_{\mathrm{F},l=1}$) contributes to the shielding on the fluorine site. Also for the perturbed wave functions, only the $\Psi_o^{(1)}|_{\mathrm{F},l=1}$ component contributes to the shielding. The observed trend of this contribution to the IS correlates with the F-2p partial charge within the metal-p bands, which is tiny for NaF but quite significant for CsF (see $Q_{\mathrm{F}-2p}$ in Table II).

The situation is more complicated for the F-p bands. As expected, only $\Psi_o^{(0)}|_{\mathrm{F},l=1}$ has to be considered for the occupied ground-state wave functions, but for the $\Psi_o^{(1)}$ both $l = 1$ and 2

TABLE II. F-2p and metal-p partial charges Q (in e^-) and major F atomic sphere contribution to the F-IS (in ppm) for the F-s, metal-p, and F-2p bands decomposed according to s, p, and d characters of $\Psi_o^{(0)}$ and $\Psi_o^{(1)}$.

	LiF	NaF	KF	RbF	CsF
			F-s		
$\Psi_o^{(0)}\|_{\mathrm{F},l=0}$	25.0	25.2	25.4	25.4	25.6
$\Psi_o^{(1)}\|_{\mathrm{F},l=1}$	25.4	27.9	25.5	25.4	25.4
			metal-p		
$\Psi_o^{(0)}\|_{\mathrm{F},l=1}$		2.6	25.4	52.5	103.2
$\Psi_o^{(1)}\|_{\mathrm{F},l=1}$		1.5	25.1	51.6	100.9
$Q_{\mathrm{F}-2p}$		0.005	0.025	0.054	0.110
			F-p		
$\Psi_o^{(0)}\|_{\mathrm{F},l=1}$	49.7	70.5	− 75.3	− 149.5	− 296.2
$\Psi_o^{(1)}\|_{\mathrm{F},l=0}$	4.5	4.5	4.6	4.8	5.0
$\Psi_o^{(1)}\|_{\mathrm{F},l=1}$	− 111.3	− 89.5	− 234.0	− 307.5	− 452.7
$Q_{\mathrm{metal}-p}$	0.117	0.063	0.092	0.146	0.223
$\Psi_o^{(1)}\|_{\mathrm{F},l=2}$	156.0	155.3	154.1	153.1	151.4

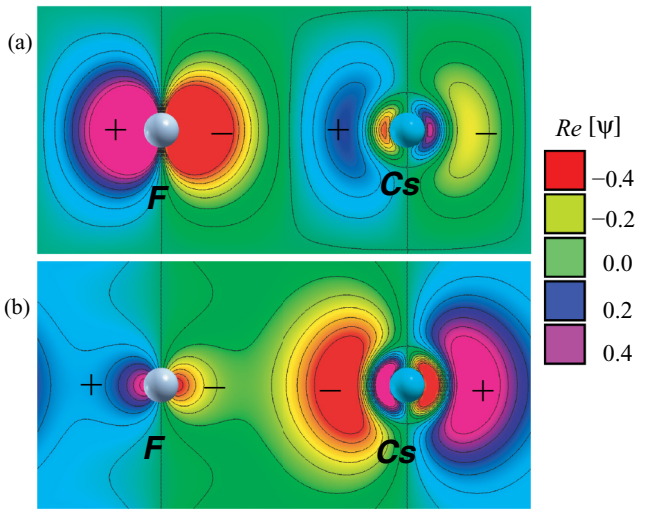

FIG. 3. (Color online) Real part of the wave function calculated at the X point for CsF. (a) The wave function corresponds to a nondegenerate state belonging to the F-p bands and clearly shows antibonding character of the Cs-p and F-p orbitals. (b) The state belongs to the Cs-p bands and is of bonding character between Cs-p and F-p orbitals.

inside F are important. The $\Psi_o^{(1)}|_{\mathrm{F},l=2}$ contributions are large but constant throughout the series, while $\Psi_o^{(1)}|_{\mathrm{F},l=1}$ contributes to the observed trend. This trend follows closely the (small) metal-p partial charges, but note that it is three to four times larger and has opposite sign than for the metal-p band. This is a result of a small but significant covalent interaction between F-p and metal-p states, which is "bonding" (same phase) in the lower metal-p band but antibonding (opposite phase) in the upper F-p band. Figure 3 illustrates the bonding (for Cs-p bands) and antibonding (for F-p bands) mixing between Cs-p and F-p states for CsF.

Apparently, the $\Psi_o^{(1)}|_{\mathrm{F},l=1}$ component has a different behavior when accompanied in Eq. (5) with F-s (constant within the series), metal-p (increasing positive contribution), or the F-p orbitals (increasing negative contribution). In order to understand this, we investigate the influence of the metal atom on the $\Psi_o^{(1)}$. For that purpose, we decompose the integral $\langle\Psi_e^{(0)}|H^{(1)}|\Psi_o^{(0)}\rangle$ entering the definition of the $\Psi_o^{(1)}$ in Eq. (6) with respect to the angular components of the empty states $\Psi_e^{(0)}$. According to Eq. (6), $\Psi_o^{(1)}$ is expanded in unoccupied states $\Psi_e^{(0)}$, and can only adopt a character that is already present in $\Psi_e^{(0)}$. However, its contribution is also controlled by the value of the integral and the energy denominator $\langle\Psi_e^{(0)}|H^{(1)}|\Psi_o^{(0)}\rangle/(\epsilon - \epsilon_e)$. Table III shows the effects of such a decomposition on the NMR shielding. For the F-s band, the interpretation is relatively simple. $\Psi_o^{(0)}$ is well localized inside the F sphere, and since it is of almost pure s character it can only couple to the F $l = 1$ character of $\Psi_e^{(0)}$. As a result, the majority character of the perturbed wave function $\Psi_o^{(1)}$ is $l = 1$, which is the only important component for the fluorine IS. It stays constant throughout the fluorides series since the occupied F-s and empty F-p states are always the same.

In the metal-p band, the majority metal-p character in $\Psi_o^{(0)}$ couples only to the metal-d character in $\Psi_e^{(0)}$, which effectively enhances the NMR active F-p component of the

TABLE III. The contribution to the fluorine IS with respect to the character of $\Psi_e^{(0)}$ entering the integral $\langle\Psi_e^{(0)}|H^{(1)}|\Psi_o^{(0)}\rangle$ from Eq. (6).

	LiF	NaF	KF	RbF	CsF
		F-s, $\Psi_o^{(1)}\|_{\mathrm{F},l=1}$			
$\Psi_e^{(0)}\|_{\mathrm{F},l=1}$	27.1	26.1	27.8	27.4	27.6
		metal-p, $\Psi_o^{(1)}\|_{\mathrm{F},l=1}$			
$\Psi_e^{(0)}\|_{\mathrm{metal},l=2}$		1.6	16.1	28.0	40.3
interstitial		0.2	10.2	26.7	68.1
		F-p, $\Psi_o^{(1)}\|_{\mathrm{F},l=1}$			
$\Psi_e^{(0)}\|_{\mathrm{metal},l=0}$	17.3	36.2	35.2	39.2	39.2
$\Psi_e^{(0)}\|_{\mathrm{metal},l=1}$	25.4	16.0	−18.5	−31.4	−44.1
$\Psi_e^{(0)}\|_{\mathrm{metal},l=2}$	17.3	−15.1	−111.3	−140.0	−160.3
$\Psi_e^{(0)}\|_{\mathrm{F},l=1}$	−479.1	−522.8	−567.6	−579.0	−604.8
interstitial	310.8	392.0	415.2	392.3	314.3
		F-p, $\Psi_o^{(1)}\|_{\mathrm{F},l=2}$			
$\Psi_e^{(0)}\|_{\mathrm{F},l=2}$	142.1	140.3	140.1	139.2	137.6

$\Psi_o^{(1)}$. Since the metal-p states are not completely confined inside the metal sphere, the interstitial region also contributes considerably to the integral $\langle\Psi_e^{(0)}|H^{(1)}|\Psi_o^{(0)}\rangle$. This indicates that there is a dependence between the position of the metal-d states and the F-IS. The energy denominator in Eq. (6) gets smaller when the unoccupied d bands get lower for heavier elements. The evolution of the metal d character across the fluorine series is displayed in Fig. 4. Thus the increase of the metal-p band contribution to the F-IS within the series comes from two contributions, namely the increased F-p admixture in the occupied states (because the metal-p band increases in energy) and the lowering of the unoccupied metal-d bands.

To some extent, the situation is inverted for the F-p bands and the $l = 1$ component of $\Psi_o^{(1)}$, besides the fact that all metal characters (namely s, p, and d) contribute to the response. However, it is still important that the small metal-p component of $\Psi_o^{(0)}$ (see Table II) couples to the metal-d character of $\Psi_e^{(0)}$. At the same time, $\Psi_e^{(0)}$ contains a large fluorine $l = 1$ component that enters the first-order perturbation $\Psi_o^{(1)}$, which due to its antibonding coupling to the metal-p states contributes more negatively in this series. The contribution to the IS related to the coupling of $\Psi_o^{(0)}|_{\mathrm{F},l=1}$ with

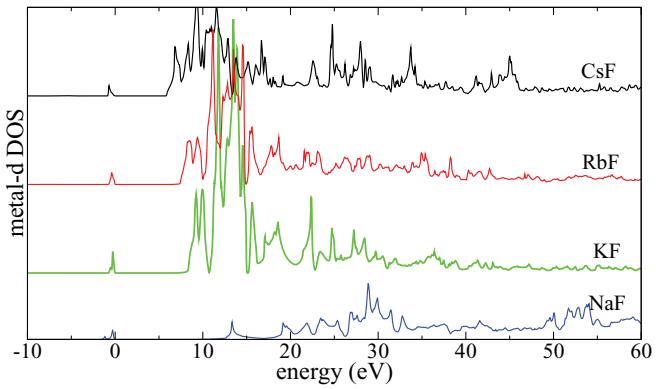

FIG. 4. (Color online) The position of the metal-d density of states across the fluoride series.

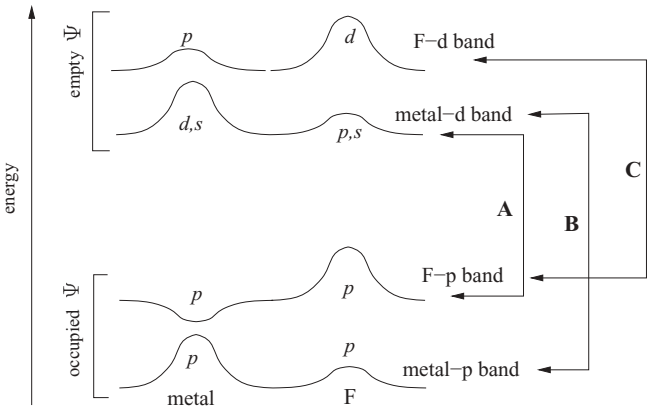

FIG. 5. Schematic diagram representing the major couplings contributing to $\Psi_o^{(1)}$. **A**, contributes to the $\Psi_o^{(1)}|_{\mathrm{F},l=1}$ component, resulting in an increasing negative contribution to the IS. **B**, also contributes to $\Psi_o^{(1)}|_{\mathrm{F},l=1}$, however it leads to an increasing positive contribution to the IS. **C**, contributes to $\Psi_o^{(1)}|_{\mathrm{F},l=2}$ resulting in a constant contribution to the IS.

$\Psi_e^{(0)}|_{\mathrm{metal},l=2}$ follows the trend determined by the evolution of the metal-d character in the fluorides series; see Fig. 4. Between KF and CsF, the change is rather moderate, however a big jump occurs between NaF and KF. Finally, the $l = 2$ component of $\Psi_o^{(1)}$ contributes with a constant fraction to the NMR shielding across the series, which is related to the coupling of the occupied $\Psi_o^{(0)}$ F-p states to the empty $\Psi_e^{(0)}$ bands with F-d character. Since the position of the F-d bands is not much affected by the specific kind of metal atom, its contribution stays constant.

This rather complex analysis can be summarized in Fig. 5. In the metal-p band, there is a small but non-negligible bonding admixture of F-p character, which increases in the series because the metal-p band gets closer to the F-p band, leading to an increased shielding. Simultaneously in the F-p band, the antibonding metal-p contribution also increases for heavier metal atoms and the shielding becomes more negative and it is the dominating effect. This interaction can also be increased when the bond length decreases, and the effect is illustrated by calculating the shielding as a function of the unit cell volume. By increasing the volume, the mixing between

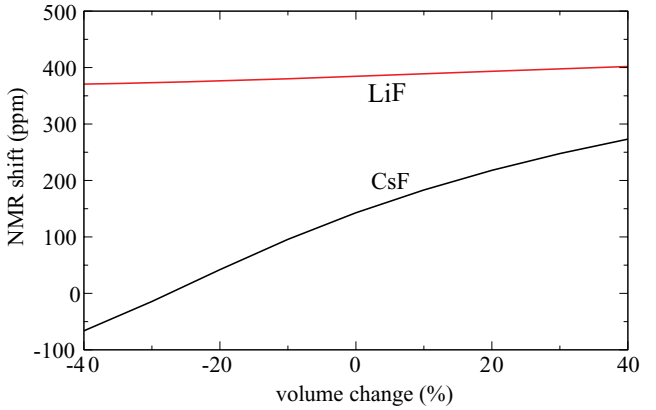

FIG. 6. (Color online) Volume dependence of the ^{19}F NMR absolute chemical shielding calculated for LiF and CsF.

TABLE IV. Effect of the LDA + U orbital potential acting on Cs-d states on the F shielding in CsF.

	$U = 0$ Ry	$U = 1$ Ry	$U = 2$ Ry	$U = 4$ Ry	$U = 8$ Ry
			F-s		
sphere	25.0	25.3	25.3	25.2	25.2
			metal-p		
sphere	103.9	83.0	71.8	59.7	49.6
$\Psi_o^{(1)}\vert_{\mathrm{F},l=1}$	100.9	81.4	70.3	58.2	48.1
			F-p		
sphere	−296.2	−179.2	−116.0	−52.1	−3.3
$\Psi_o^{(1)}\vert_{\mathrm{F},l=1}$	−452.7	−336.1	−273.1	−209.6	−160.0
$\Psi_o^{(1)}\vert_{\mathrm{F},l=2}$	151.4	152.0	152.3	152.6	156.2
total (+ core)	142.6	241.0	291.0	343.7	382.2

metal-p and F-p characters decreases and effectively increases the fluorine shielding. The effect is large for CsF; see Fig. 6. However, it is small for compounds where the interaction between metal-p and F-p states is small, e.g., in a case in which the energy separation is already large, as in LiF and NaF (Fig. 6).

The second important ingredient in the trend comes from the perturbation of the wave function $\Psi_o^{(1)}$, which is generated by a coupling of the occupied bands to the empty states. The F-d bands stay more or less constant in this series, while the metal-d bands come closer to the occupied bands and the negative IS contribution increases [via the energy denominator in Eq. (6)] and thus dominates the variation of the observed IS. Such effects are demonstrated by DFT + U calculations,[27] where the d states can be shifted artificially by an external orbital potential. The value of the shielding is controlled by the parameter U. Table IV presents the NMR shielding as well as its major contributions as a function of U calculated for CsF. Naturally, the contribution from the F-s band is not affected by the orbital potential because in this case the metal-d character does not participate in $\Psi_o^{(1)}\vert_{\mathrm{F},l=1}$. The contribution coming from the Cs-p bands, however, decreases gradually with increasing U, which agrees with our previous conclusion that the metal-d states take an active part in the formation of $\Psi_o^{(1)}\vert_{\mathrm{F},l=1}$. Since the F-$p$ admixture in the ground state is not changed, we cannot decrease the metal-p contribution to zero (as it is for LiF and NaF). For the F-p bands, the absolute value of the shielding related to the $\Psi_o^{(1)}\vert_{\mathrm{F},l=1}$ decreases as expected by about the same amount as the $\Psi_e^{(0)}\vert_{\mathrm{metal},l=2}$ component. On the other hand, the component related to $\Psi_o^{(1)}\vert_{\mathrm{F},l=2}$ is not affected by U because the Cs-d character does not participate in the response.

IV. CONCLUSIONS

To conclude, we have performed a detailed analysis of the relation between NMR shielding and electronic structure for a series of alkali fluorides. Our goal was to understand the origin of the observed trend. We have shown that the F-p band contributions are essential but the metal-p bands cannot be neglected. It is interesting to note that both sets of bands result in an opposite variation of the shielding throughout the series. The metal-p part of the shielding is positive and increases from light to heavy metal compounds, whereas for the F-p bands the shielding is negative for heavier elements and decreases through the series. We have indicated that for both sets of bands the (small) covalent bonding and antibonding interaction between metal-p and F-p states is essential, but the metal-d character (present in the unoccupied part of the spectrum) is also a key component in the first-order perturbation of the occupied KS states.

With this analysis, we can explain the origin and the trends observed in NMR experiments. It can also be applied to other materials and nuclei. For instance, we have already looked into more complex fluorides or the oxygen NMR shielding parameters of several (ionic) oxides, where very similar trends were observed.

ACKNOWLEDGMENTS

We thank Monique Body (Universitè du Maine) for fruitful discussions. We would like to acknowledge support by the Austrian Science Foundation (FWF) under project SFB-F41 (ViCoM).

[1] *Calculation of NMR and EPR Parameters. Theory and Applications*, edited by M. Kaupp, M. Bühl, and V. G. Malkin (Wiley, New York, 2004).

[2] *Encyclopedia of NMR*, edited by C. M. Grant and R. K. Harris (Wiley, New York, 1996).

[3] M. Schindler, J. Am. Chem. Soc. **109**, 1020 (1987).

[4] B. Bureau, G. Silly, J. Buzaré, and J. Emery, Chem. Phys. **249**, 89 (1999).

[5] M. Body, G. Silly, C. Legein, and J.-Y. Buzaré, Inorg. Chem. **43**, 2474 (2004).

[6] M. Body, G. Silly, C. Legein, J.-Y. Buzaré, F. Calvayrac, and P. Blaha, J. Solid State Chem. **178**, 3655 (2005).

[7] C. Martineau, M. Body, C. Legein, G. Silly, J.-Y. Buzaré, and F. Fayon, Inorg. Chem. **45**, 10215 (2006).

[8] C. M. Widdifield and D. L. Bryce, J. Phys. Chem. A **114**, 2102 (2010).

[9] P. d'Antuono, E. Botek, B. Champagne, J. Wieme, M.-F. Reyniers, G. B. Marin, P. J. Adriaensens, and J. M. Gelan, J. Phys. Chem. B **112**, 14804 (2008).

[10] C. Legein, F. Fayon, C. Martineau, M. Body, J.-Y. Buzare, D. Massiot, E. Durand, A. Tressaud, A. Demourgues, O. Peron *et al.*, Inorg. Chem. **45**, 10636 (2006).

[11] C. Martineau, C. Legein, J.-Y. Buzare, and F. Fayon, Phys. Chem. Chem. Phys. **11**, 950 (2009).

[12] A. Sadoc, M. Body, C. Legein, M. Biswal, F. Fayon, X. Rocquefelte, and F. Boucher, Phys. Chem. Chem. Phys. **13**, 18539 (2011).

[13] A.-L. Rollet, M. Allix, E. Veron, M. Deschamps, V. Montouillout, M. R. Suchomel, E. Suard, M. Barre, M. Ocaa, A. Sadoc *et al.*, Inorg. Chem. **51**, 2272 (2012).

[14]K. Schwarz and P. Blaha, Z. Naturforsch. **47a**, 197 (1992).
[15]D. S. Middlemiss, F. Blanc, C. J. Pickard, and C. P. Grey, J. Magn. Reson. **204**, 1 (2010).
[16]U. Gross, S. Rüdiger, A.-R. Grimmer, and E. Kemnitz, J. Fluor. Chem. **115**, 193 (2002).
[17]J. M. Miller, Prog. Nucl. Magn. Reson. Spectrosc. **28**, 255 (1996).
[18]S. Hayashi and K. Hayamizu, Bulletin of the Chemical Society of Japan **63**, 913 (1990).
[19]A. Zheng, S.-B. Liu, and F. Deng, J. Phys. Chem. C **113**, 15018 (2009).
[20]M. Body, G. Silly, C. Legein, and J.-Y. Buzaré, J. Phys. Chem. B **109**, 10270 (2005).
[21]R. Laskowski and P. Blaha, Phys. Rev. B **85**, 035132 (2012).
[22]F. Mauri, B. G. Pfrommer, and S. G. Louie, Phys. Rev. Lett. **77**, 5300 (1996).
[23]C. J. Pickard and F. Mauri, Phys. Rev. B **63**, 245101 (2001).
[24]J. R. Yates, C. J. Pickard, and F. Mauri, Phys. Rev. B **76**, 024401 (2007).
[25]P. Blaha, K. Schwarz, G. K. H. Madsen, D. Kvasnicka, and J. Luitz, *WIEN2k, An Augmented Plane Wave Plus Local Orbitals Program for Calculating Crystal Properties* (Vienna University of Technology, Vienna, 2001).
[26]J. P. Perdew, K. Burke, and M. Ernzerhof, Phys. Rev. Lett. **77**, 3865 (1996).
[27]V. I. Anisimov, I. V. Solovyev, M. A. Korotin, M. T. Czyżyk, and G. A. Sawatzky, Phys. Rev. B **48**, 16929 (1993).